Fundamental Study of Water-Gas Shift Reaction in Ironmaking Process

M. Bahgat*[1], K. S. Abdel Halim[2], H. A. El-Kelesh[3], M. I. Nasr[4]
Central Metallurgical Research and Development Institute (CMRDI),
P.O.Box 87-Helwan, Cairo, 11421, Egypt
*[1]M_bahgat70@yahoo.com; [2]khsaad99@yahoo.com; [3]Heba_chemist2004@yahoo.com; [4]minasr@hotmail.com

***Abstract*- The iron and steel industry is emitting about 2 billion tons of CO_2 per year. Enhancement of iron oxide reducibility will decrease coke consumption and CO_2 emission. The water–gas shift reaction plays a significant role in the reduction of iron oxides to iron in the blast furnace. So, the fundamental study of water-gas shift reaction is very important.**

Wustite samples were prepared from reagent grade hematite by gaseous reduction with 50%CO-CO_2 gas mixture at 1000°C. Using thermogravimetric technique, wustite samples were isothermally reduced at 800-1100°C by different ratios of $H_2/CO/CO_2/N_2$. The influences of temperature and gas composition on the reduction behavior and the morphology were investigated. In case of lower total reducing gas concentration 50%, water-gas phenomena takes place under the effect of both temperature and H_2 concentration. The reduction rate increased with H_2 concentration at higher temperature but decreased with H_2 concentration at lower temperature due to water gas shift reaction. Lower temperature and hydrogen gas concentration are both the preferable conditions for water-gas shift reaction phenomena to have an influence.

Keywords- Water-Gas Shift Reaction; Iron Making; CO_2 Emissions; Blast Furnace; Wustite Reduction

I. INTRODUCTION

The iron and steel industry is emitting about 2 billion tons of CO_2 per year. Enhancement of iron oxide reducibility will decrease coke consumption and CO_2 emission. The water–gas shift reaction plays a significant role in the reduction of iron oxides to iron in the blast furnace. So, the fundamental study of water-gas shift reaction is very important.

Some previous investigations studied water-gas shift reaction [1-5]. Influence of water–gas shift reaction on wustite reduction was investigated by Wang et al. [1]

$$CO_2\,(g) + H_2\,(g) = CO\,(g) + H_2O\,(g)$$
$$\Delta H = 41\,325\ J/mol$$

This reaction is reversible and has high reaction rate above 800°C. Introducing a small quantity of hydrogen into gas mixture accelerates the reduction process because the product H_2O reacts with CO to create H_2, which takes part in the reduction again. Part of H_2 does not participate in the reduction, but it acts as something like catalyzer which speeds up the reduction greatly.

If concentrations of H_2 and CO_2 are both high in gas mixture, the water–gas shift reaction tends to shift to the right direction which leads to the decrease of H_2 and enhancement of CO and H_2O. The reducing power of gas mixture is then weakened.

The water–gas shift reaction counteracts wustite reduction in the case of gas mixture with high content of CO_2 and H_2 at elevated temperature.

The water–gas shift reaction plays a significant role in the reduction of iron oxides to iron in the blast furnace and in direct reduction processes when hydrogen is present in the reducing agent for (FeO) than CO [2]. Thus, wustite is reduced largely by H_2, and a major use for the CO is to regenerate H_2. Water-gas shift reaction must be catalyzed to be effective at temperatures of iron oxide reduction; therefore, it is of interest to determine its mechanism on iron and iron oxide catalyst surfaces.

Takeaki Murayama [3] studied the effect of water gas shift reaction on the reduction theoretically and experimentally in the fixed bed reduction of wustite pellets with H_2–CO and H_2- CO_2 gas mixtures at 900°C. In the model analysis, the water gas shift reaction, the effect of high void fraction in the peripheral part of the fixed bed next to the reaction tube wall on the gas flow, the effect of the gas composition on the parameters, the oxygen diffusion in the dense iron layers, and the heat of reactions were taken into account. In the reduction with H_2–CO, the effect of water gas shift reaction on the reduction curves was not so significant. However, the temperature in the bed was lowered slightly by the effect of heat of the reaction. In the reduction with H_2–CO_2, the effect of water gas shift reaction on the reduction becomes significant with an increase of CO_2 composition in the inlet gas. The temperature in the bed was lowered remarkably.

In the present investigation, reduction behaviour of synthesised pure chemical wustite was studied at 800–1100°C using different ratios of $H_2/CO/CO_2/N_2$ gas mixture to clarify the water gas shift reaction phenomena and its effect inside the blast furnace during ironmaking process.

II. EXPERIMENTAL

In the present study, pure wüstite samples were used for the experiments. The pure wustite samples were prepared by reduction of pure hematite. A reagent grade (A.R) hematite powder (99.9%) was compacted in a cylinderical shape. These compacts were sintered at 1200°C in air for 24 hrs. After that the sintered compacts were crushed and reduced to wüstite using a CO/CO_2 gas mixture at a ratio of 1/1 in a total flow rate of 1 l/min at 1000°C. Due to the non-stoichiometric character of the wüstite, the reaction was extended, after the initial reduction, for about 6 hrs to assure the homogeneous

structure distribution of the cation vacancies and holes on the formed wüstite. Pure wüstite powders were compacted into briquettes of about 1 gm weight, 7 mm diameter and 5 mm height.

The prepared wustite samples were then reduced in thermogravimetric apparatus at 800-1100°C by different ratios of $H_2/CO/CO_2/N_2$. The reduction assembly and gas flow system used in this study were previously mentioned [6].

The course of reduction was followed up by measuring the weight loss as a function of time under controlled conditions of temperature and gas composition. For each reduction experiment, the furnace was heated up to the required reduction temperature, and then the sample was weighed and placed in a platinum wire basket. The sample was then gradually introduced into the furnace so as to avoid thermal shock cracking and positioned in the middle of the furnace constant hot zone. First, nitrogen at a flow rate of 1 liter/min was introduced. After the sample soaking for 10 min at the reduction temperature, the reducing gas mixture at a flow rate of 1 liter/min was introduced. The weight loss resulting from oxygen removal from the briquettes was intervally recorded with time. At the end of the experiment, the basket with the reduced briquettes was removed and dropped by releasing its suspension wire from the balance, into a conical flask containing acetone to prevent pyrophority of the reduced sample.

The fired and reduced samples were examined with the aid of reflected light microscope (Meiji CK 3900), scanning electron microscope (JEOL, JSM-5410), X-ray diffraction analysis (JSX-60P JEOL diffractometer with a copper target) and pore size distribution (Micromeritics Pore Sizer 9320).

III. RESULTS and DISCUSSIONS

A. Characterization of Prepared Wüstite Samples

The annealed pure wüstite compacts were characterized with XRD analysis. It was found that the wüstite phase is clearly displayed in XRD charts as shown in the XRD pattern in Fig. 1. From XRD analysis the average crystallite size was calculated using the diffractions peaks from Scherer's formula as shown below:

$$D = 0.9 \lambda / \beta \cos \theta \qquad (3.1.1)$$

Where D is the crystallite size, λ the X-ray wavelength, β the broadening of the diffraction peak and θ is the diffraction angle [7]. It was found that the crystalline size is 85.4 nm.

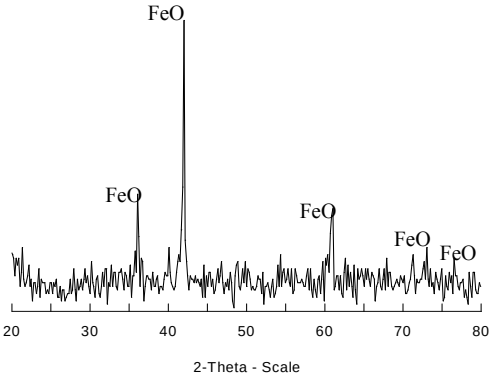

Fig. 1 XRD analysis for prepared pure wüstite

Figure 2 shows the SEM micrographs for annealed pure wustite. It was observed that the grains are formed in pellet shape and grain coalescence with large number of both macro- and micropores took place.

Also, pure wustite samples were examined by optical microscope. The microstructure of pure wüstite compacts is a matrix of globular wüstite grains forming porous structure with homogeneously distributed macro- and micro-pores.

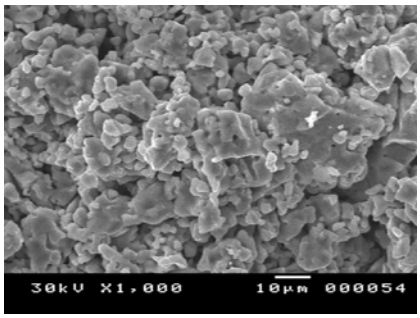

Fig. 2 SEM micrograph of annealed pure wustite sample

B. Reduction Behavior of Wustite Samples

Using thermo-gravimetric technique, pure wustite samples were isothermally reduced at the temperature range 800-1100°C by different ratios of $H_2/CO/CO_2/N_2$ (Table I) with different reducing gases ratios whereas $H_2/(H_2+CO)$= 0.33 and 0.67 for total reducing gases ratio $(H_2+CO)/(H_2+CO+CO_2+N_2)$= 0.9 and $H_2/(H_2+CO)$= 0.4 and 0.6 for total reducing gases ratio $(H_2+CO)/(H_2+CO+CO_2+N_2)$= 0.5. Although these ratios are not equal to the actual values inside the blast furnace, they were used to clarify the water gas shift reaction phenomena at the temperature range 800-1100°C. The reduced samples were characterized by XRD. It was found that wüstite is reduced gradually to metallic iron. The influence of reduction temperature and reducing gases composition on the reduction behavior and structural characteristics of the reduced products was studied in order to elucidate the kinetics and mechanisms of reduction.

TABLE I THE VARIOUS GAS COMPOSITIONS APPLIED for ISOTHERMAL REDUCTION of WUSTITE SAMPLES.

Gas composition, vol%				$H_2/(H_2+CO)$	$(H_2+CO)/(H_2+CO+CO_2+N_2)$	Temp.,°C
H_2	CO	CO_2	N_2			
30	60	10	---	0.33	0.9	800-1100
60	30	10	---	0.67		
20	30	10	40	0.4	0.5	
30	20	10	40	0.6		

1) Effect of Temperature:

The isothermal reduction curves of wüstite compacts reduced by $(H_2+CO)/(H_2+CO+CO_2+N_2)$= 0.9 and 0.5 at 800-1100°C are given in Figs. 3 and 4 respectively. For each single reduction curve, the rate of reduction was the highest at the early stages and decreased as reduction proceeds till the end of reduction. The reduction mainly came to its completion for

all samples reduced by all gas compositions at 800-1100°C. The effect of temperature on the rate of reduction has a characterized behavior that for $(H_2+CO)/(H_2+CO+CO_2+N_2)$ = 0.9, the reaction rate normaly increased with increasing temperature. On the other hand, for $(H_2+CO)/(H_2+CO+CO_2+N_2)$ = 0.5 the reaction rate becomes independent on reduction temperature whereas the reduction rate did not increase gradually with increasing temperature especially at low H_2 concentration. This phenomenon is due to the possibility of introducing water-gas shift reaction.

$$H_2 + CO_2 \xrightarrow{800^oC} CO + H_2O$$

The equilibrium of this reaction is at 800°C. At higher temperatures the reaction shifts to the direction of CO formation which makes the percent of CO higher than H_2 in the medium i.e. H_2 is consumed in reaction with CO_2 rather than reducing wustite. Since CO has reducing power lower than H_2. So, reduction extent decreases gradually with the proceeding time by increasing the reduction temperature.

The microstructure for pure compacts reduced by $H_2/(H_2+CO)$ = 0.6 at 900 and 1100°C is examined by optical microscope. It is found that metallic iron is homogenously distributed in a structure with large number of macro- and micro-pores which allows for a good access of reducing gas to wüstite grains.

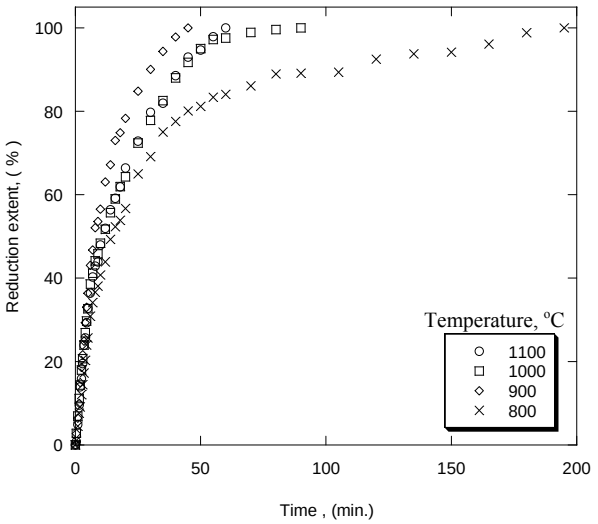

Fig. 4 Effect of temperature on the reduction behaviour of wustite reduced by $H_2 / (H_2 + CO)$ = 0.4 with total reducing gas ratio 0.5

At both lower and higher reducing gases ratios $(H_2+CO)/(H_2+CO+CO_2+N_2)$= 0.5 and 0.9, the total porosity decreases by increasing reduction temperature as shown in Table II.

TABLE II TOTAL POROSITY for WUSTITE SAMPLES REDUCED by DIFFERENT GAS COMPOSITIONS at 900 and 1100°C

Temp.°C	Total porosity, %			
	$(H_2+CO)/(H_2+CO+CO_2+N_2)$= 0.9		$(H_2+CO)/(H_2+CO+CO_2+N_2)$= 0.5	
	$H_2/(H_2+CO)$= 0.33	$H_2/(H_2+CO)$= 0.67	$H_2/(H_2+CO)$= 0.4	$H_2/(H_2+CO)$= 0.6
900 °C	47.0	46.37	53.65	51.82
1100 °C	46.34	45.36	48.01	39.26

Figure 5 shows the relation between incremental pore volume and pore diameter for wustite compacts reduced by $H_2/(H_2+CO)$ = 0.67 for total reducing gas ratio $(H_2+CO)/(H_2+CO+CO_2+N_2)$ = 0.9 at 900 and 1100°C respectively. It can be noticed that The incremental intrusion value for the sample reduced at 900°C is slightly higher than that for the sample reduced at 1100 °C, which reflects increasing of pore size and pore number by decreasing reduction temperature and is also confirmed by SEM micrographs for wustite samples reduced by $H_2/(H_2+CO)$ = 0.67 for total reducing gas ratio $(H_2+CO)/(H_2+CO+CO_2+N_2)$ = 0.9 at 900 and 1100°C respectively.

The structure of the sample reduced at 900°C indicates relatively small grains but by increasing temperature the grains tended to be larger and connected to each other forming relatively more dense structure with lower porosity. This result was obtained from wustite samples reduced by $H_2/(H_2+CO)$ = 0.4 for total reducing gas ratio $(H_2+CO)/(H_2+CO+CO_2+N_2)$ = 0.5 at 900 and 1100°C as shown in Fig. 6 (a and b) respectively. It can be noticed that structure densification takes place by increasing reduction temperature from 900°C to 1100°C.

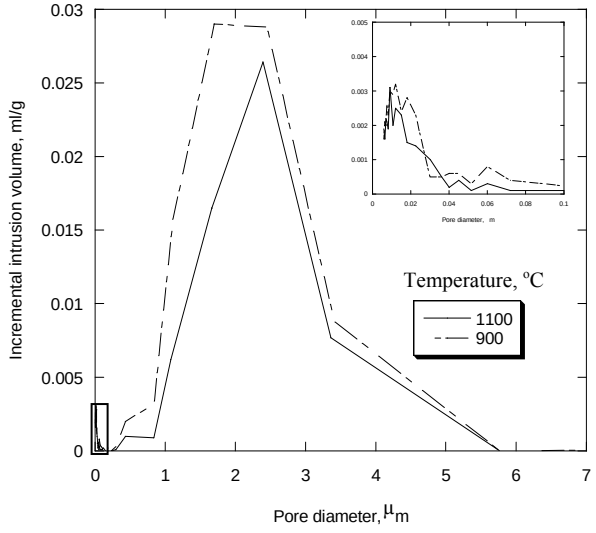

Fig. 5 The pore size distribution for samples reduced by $H_2/(H_2+CO)$ = 0.67 with total reducing gas ratio 0.9 at 900 and 1100°C

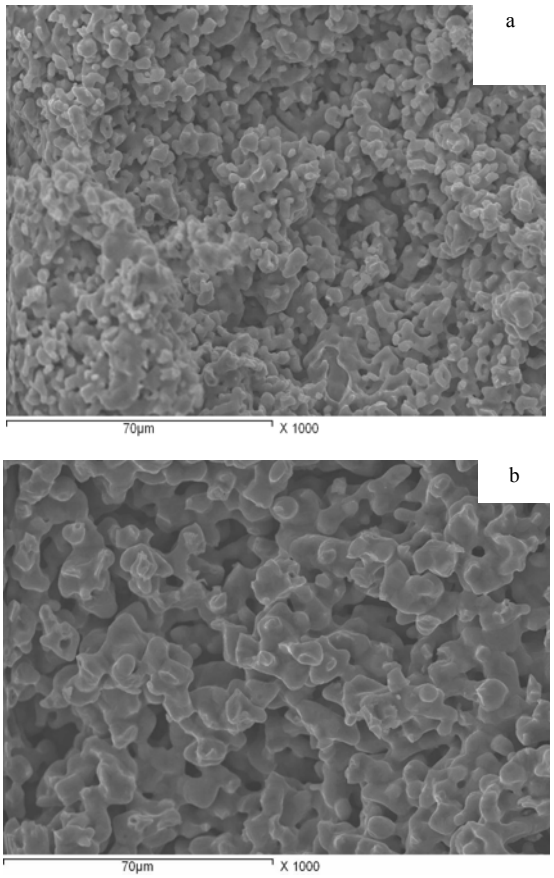

Fig. 6 SEM micrographs of wustite samples reduced by $H_2/(H_2+CO)$ = 0.4 with total reducing gas ratio 0.5 at :

a) 900ºC b) 1100ºC

2) Effect of Reducing Gas Composition:

The isothermal reduction curves of wüstite compacts reduced by $(H_2+CO)/(H_2+CO+CO_2+N_2)$= 0.5 and 0.9 at 900 and 1000ºC are given in Figs. 7 and 8 respectively. The reduction rate increased by increasing total reducing gas ratio $(H_2+CO)/(H_2+CO+CO_2+N_2)$ from 0.5 and 0.9. For samples reduced by $(H_2+CO)/(H_2+CO+CO_2+N_2)$ = 0.9, the reduction rate increased with H_2 concentration either at higher or lower temperatures.

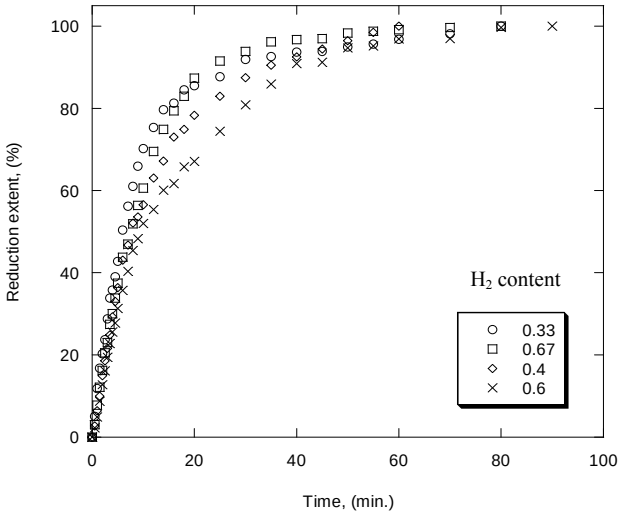

Fig. 7 Effect of reducing gas ratios on the reduction behavior of wustite at 900ºC

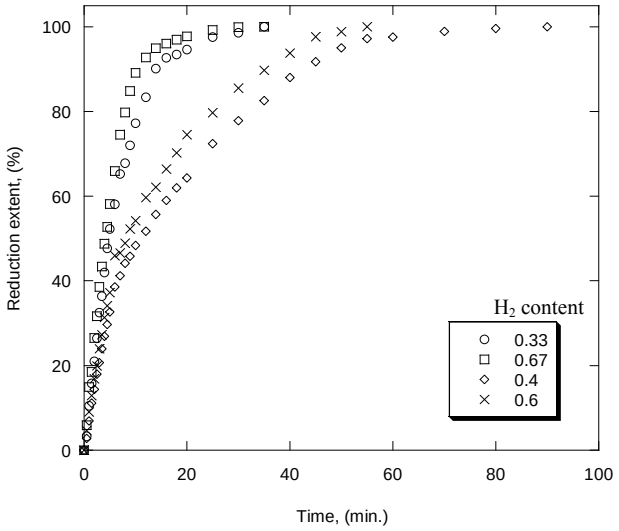

Fig. 8 Effect of reducing gas ratios on the reduction behavior of wustite at 1000ºC

For samples reduced by $(H_2+CO)/(H_2+CO+CO_2+N_2)$ = 0.5, the reduction rate increased with H_2 concentration at higher temperatures but decreased with H_2 concentration at lower temperatures due to effect of water gas shift reaction. By increasing H_2 concentration in reducing gas the water gas shift reaction shifted toward the direction of CO formation so the rate of reduction decreased due to the lower reduction strength of CO compared to that of H_2.

The difference between reduction rates of samples reduced by $(H_2+CO)/(H_2+CO+CO_2+N_2)$= 0.5 and 0.9 decreased by decreasing reduction temperature.

Figure 9 shows the relation between incremental pore volume and pore diameter for wustite compacts reduced by $H_2/ (H_2+CO)$ = 0.4 and 0.6 at 1100ºC. It can be noticed that the incremental intrusion value for the sample reduced with H_2 gas ratio 0.4 is higher than that with 0.6 and it has greater number of macro- and micro-pores. This means that pore number increased by decreasing H_2 gas concentration in reducing gas. This is confirmed by optical microscope.

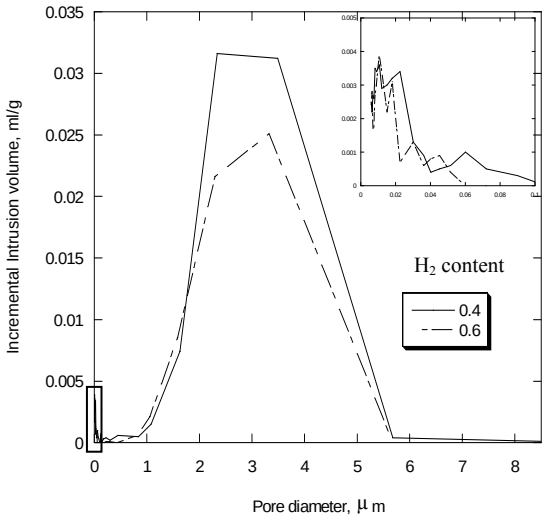

Fig. 9 The pore size distribution for samples reduced by total reducing gas ratio 0.5 at 1100ºC

It can be noticed that by increasing H_2 concentration the produced metallic structure relatively becomes denser for both total reducing gas ratios 0.5 and 0.9. This can be attributed to the relatively higher reaction rate at higher H_2 concentration which leads to accumulation of metallic particles and densification takes place.

The microstructure of wustite samples reduced by H_2/ (H_2+CO) = 0.4 and 0.6 with total reducing gas ratio 0.5 at 1100°C was examined by scanning electron microscope as shown in Fig. 10 (a and b) respectively. It can be observed that samples reduced by lower H_2 concentration has relatively small and separated grains with higher number of pores whereas by increasing H_2 concentration grains become larger and agglomerated to each other with lower number of pores.

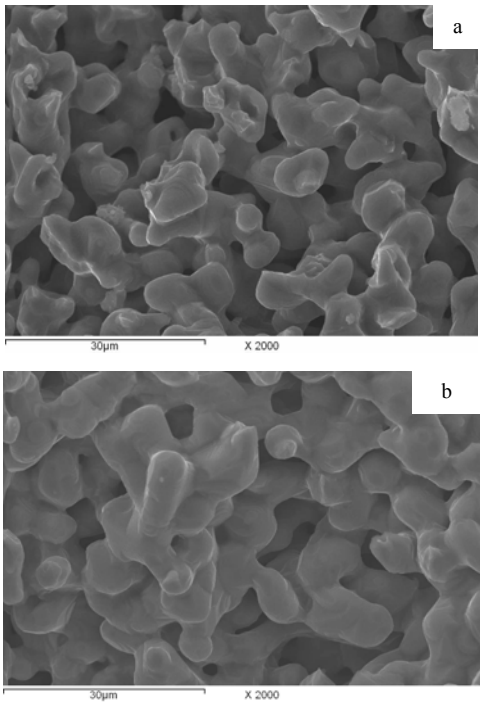

Fig. 10 SEM micrographs of wustite samples reduced at 1100°C by total reducing gas ratio 0.5 with H_2/(H_2+CO) = :
a) 0.4 b) 0.6

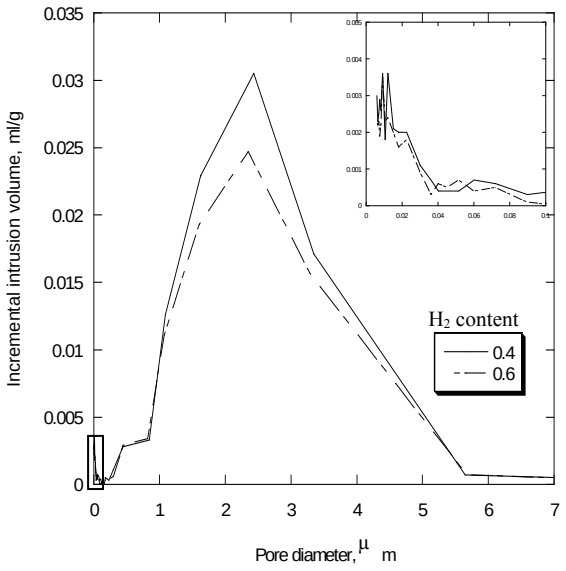

Fig. 11 The pore size distribution for samples reduced by total reducing gas ratio 0.5 at 900°C

On the other hand, the total porosity decreases from 53.65% to 51.82% by increasing H_2 gas concentration from 0.4 to 0.6 respectively for total reducing gas ratio 0.5. Figure 11 shows the relation between incremental pore volume and pore diameter for wustite compacts reduced by H_2/(H_2+CO) = 0.4 and 0.6 with total reducing gas ratio 0.5 at 900°C. It can be noticed that the incremental intrusion values increased by decreasing the H_2 percent in reducing gas composition which reflects that the samples reduced by lower H_2 percents have higher number of macro and micro-pores. That is because by increasing H_2 concentration in reducing gas composition the reduction rate decreased due to water gas shift reaction phenomena so densification takes place in the structure of samples with lower reduction rate.

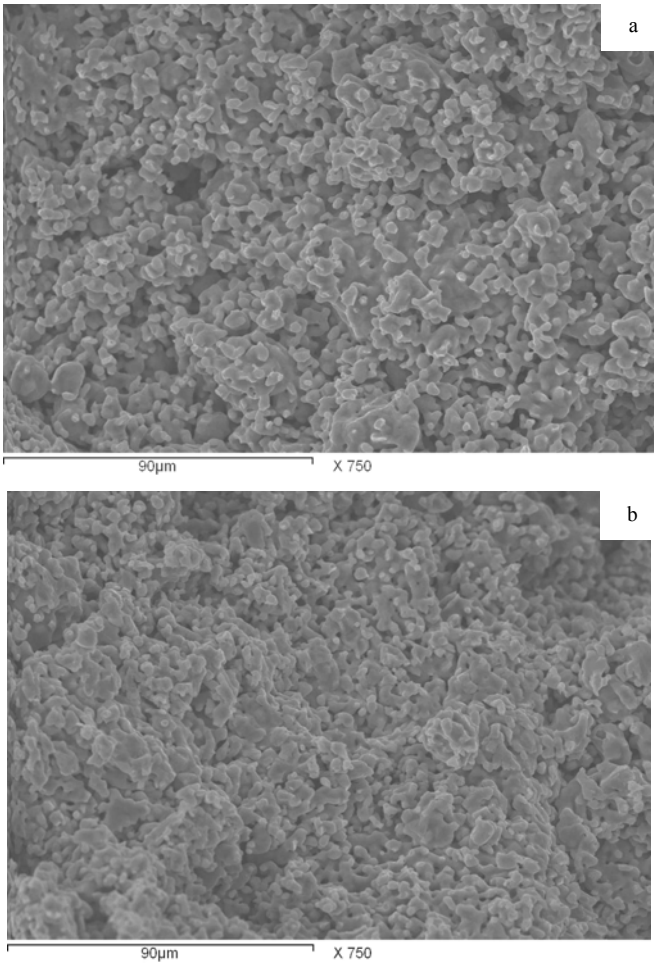

Fig. 12 SEM micrographs of wustite samples reduced at 900°C by total reducing gas ratio 0.9 with H_2/(H_2+CO) = :
a) 0.33 b) 0.67

Figure 12 (a and b) for compacts reduced by H_2/ (H_2+CO) = 0.33 and 0.67 for total reducing gas ratio 0.9 at 900°C shows that at lower reaction temperature grains become connected with each other and porosity decreased by increasing H_2 concentration in reducing gas.

Also, the internal structure of different samples reduced by H_2/ (H_2+CO) = 0.4 and 0.6 with total reducing gas ratio 0.5 at constant temperature (900°C) is examined by optical microscope as shown in Fig. 13 (a and b) respectively. It can be noticed that the produced metallic iron had a dense structure at higher H_2 concentration while at lower H_2 concentration porous structure was formed.

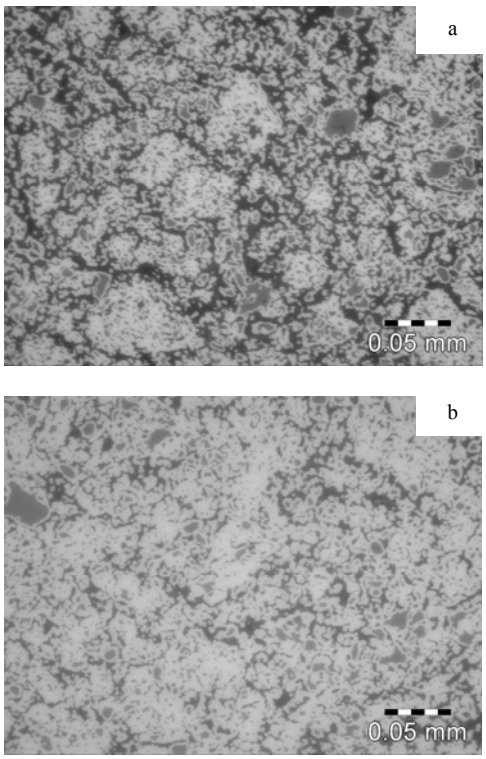

Fig. 13 Microstructure photos of wustite samples reduced at 900 ºC by total reducing gas ratio 0.5 with H_2 / (H_2 + CO) =:
a) 0.4 b) 0.6 (x=400)

C. Rate Controlling Steps and Reduction Mechanisms

In order to predict the rate controlling mechanism at both the initial and final stages of reduction, the values of apparent activation energy (E_a) were calculated from Arrhenius equation Eq. (1):

$$K_r = K_o\, e^{-Ea/RT} \qquad (3.3.1)$$

Where K_r is the reduction rate constant, K_o is the frequency factor, R is the gas constant and T is the absolute temperature. The application of different heterogeneous gas-solid mathematical models and the internal structure of partially reduced compacts were examined and correlated with each other.

The relationships between the logarithm of the rate of reduction (dr/dt) and the reciprocal of the absolute temperature 1/T are plotted at both initial (20%) and final (80%) reaction stages for wüstite samples reduced by $H_2/(H_2+CO)$= 0.4 and 0.6 with total reducing gas ratio $(H_2+CO)/(H_2+CO+CO_2+N_2)$= 0.5.

From the obtained results, the apparent activation energy (E_a) is calculated at the initial and final stages as shown in Table III:

TABLE III THE APPARENT ACTIVATION ENERGY (EA) VALUES CALCULATED at the INITIAL and FINAL REDUCTION STAGES for WÜSTITE SAMPLES REDUCED by DIFFERENT RATIOS of REDUCING GAS.

Reaction stage / % of reducing gas	Ea values at different ratios of $H_2/(H_2+CO)$ with total reducing gas ratio $(H_2+CO)/(H_2+CO+CO_2+N_2)$= 0.5, (kJ/mole)	
	= 0.4	= 0.6
Initial	38.21	42.98
Final	64.67	66.87

The values of activation energy indicate the type of mechanism by comparing them with Table IV [8]:

TABLE IV RELATIONSHIP BETWEEN ACTIVATION ENERGY VALUES (EA) and THE RATE CONTROLLING STEP.

Activation energy value, Ea (KJ/mol)	Probable rate controlling step
8-16	Gas diffusion
29-42	Combined gas diffusion and interfacial chemical reaction
60-67	Interfacial chemical reaction
› 90	Solid- state diffusion

The calculated activation energy values indicate that the reduction at the initial stages for wüstite reduced by $H_2/(H_2+CO)$ = 0.4 and 0.6 with total reducing gas ratio 0.5 are most likely controlled by combined effect of both gaseous diffusion and interfacial chemical reaction mechanisms while at the final reduction stages it is most likely controlled by interfacial chemical reaction mechanism.

In order to confirm the validity of the reduction mechanism, the following mathematical formulations Eqs. (2-4) derived by Szekely et al. [9-12] were tested against the experimental results:

(1) $t^* = (P_F(X)) = X + (1-X)\ln(1-X)$ (3.3.2)

For gaseous diffusion mechanism

(2) $t^* = (G_F(X)) = 1-(1-X)^{0.5}$ (3.3.3)

For chemical reaction mechanism

(3) $t^* = G_F(X) + \sigma^2 P_F(X)$ (3.3.4)

For the mixed control mechanism

Where X = fractional reduction degree,

t^* = dimensionless time,
σ = gas-solid reaction modulus.

By applying the different mathematical formulations derived from gas-solid reaction model, it was found that straight lines were obtained on applying the mixed control of the chemical reaction and gaseous diffusion mechanism at the initial reaction stages of wustite samples reduced by $H_2/(H_2+CO)$ = 0.4 and 0.6. Also the straight lines were obtained on applying the chemical reaction mechanism at the final reaction stages of all samples. This was in good agreement with the suggested controlling mechanisms from the calculated activation energy values at both initial and final reduction stages for all samples.

The microstructure of wüstite compacts partially reduced (20%) by $H_2/(H_2+CO)$ = 0.6 with total reducing gas ratio 0.5 at 1000°C was examined by reflected light microscope as shown in Fig. 14-a. It was observed that some micro and macropores were observed in homogenous distribution with the produced metallic iron and wustite grains that reflected the ability of gas access and successful iron nucleation in these samples. At the same time, dense structure of connected wustite grains was detected.

So, both gaseous diffusion and interfacial chemical reaction mechanisms are controlling the reaction as concluded above by Ea calculations.

The microstructure of pure wüstite compacts partially reduced (80%) by $H_2/(H_2+CO) = 0.6$ with total reducing gas ratio 0.5 at 1000°C was examined by reflected light microscope as shown in Fig. 14-b. It was observed that the formed metallic iron structure looked relatively porous with the presence of many micro and macro-pores in homogeneous distribution for all samples. These observations confirm the concluded reaction controlling mechanisms by Ea calculations.

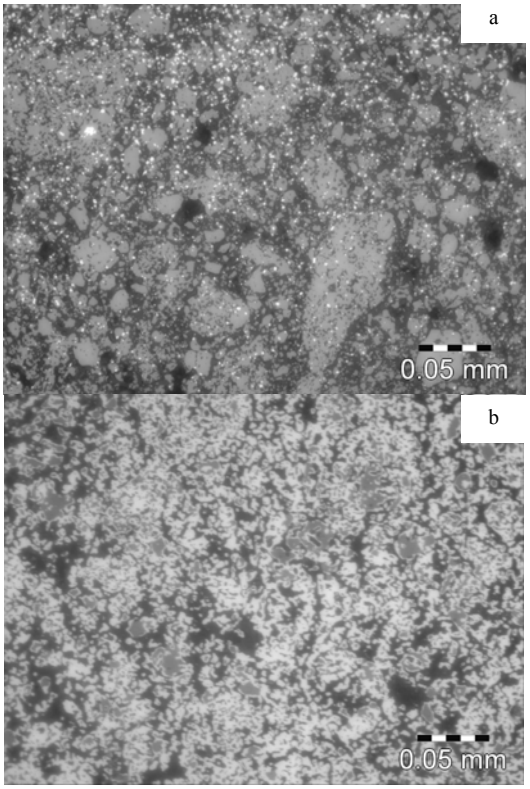

Fig. 14 Photomicrographs of samples partially reduced to various reduction extents at 1000 °C by $H_2 / (H_2+CO) = 0.6$ with total reducing gas ratio 0.5:

a) 20% b) 80% (x= 400)

IV. CONCLUSIONS

1- Wüstite samples were isothermally reduced at 800-1100°C by different ratios of $H_2/CO/CO_2/N_2$.
2- For $(H_2+CO)/(H_2+CO+CO_2+N_2)= 0.9$, The reduction rate of wustite samples normaly increased with increasing either temperature or H_2 gas concentration.
3- For $(H_2+CO)/(H_2+CO+CO_2+N_2)= 0.5$, the reaction rate becomes independent on reduction temperature specially at low H_2 concentration due to water gas shift reaction. Also, the reduction rate increased with H_2 concentration at higher temperature but decreased with H_2 concentration at lower temperature due to water gas shift reaction.
4- At both lower and higher reducing gases ratios, the total porosity decreases by increasing reduction temperature from 800 to 1100°C.
5- At both lower and higher reduction temperature, the total porosity for reduced product decreases by increasing H_2 gas concentration for both total reducing gas ratios 0.5 and 0.9.
6- The reduction rate of samples at the initial stages it is most likely controlled by the combined effect of chemical reaction and gaseous diffusion mechanisms while at the final stages it is most likely controlled by interfacial chemical reaction mechanism.
7- In case of high total reducing gas ratio (0.9), water gas shift reaction phenomena does not take place either at low or high temperature and H_2 concentration.
8- In case of lower total reducing gas ratio (0.5), water-gas phenomena takes place under the effect of both temperature and H_2 concentration
9- Lower temperature and hydrogen gas concentration are both the preferable conditions for water-gas shift reaction phenomena to take place.

ACKNOWLEDGMENT

This work is fully supported by the Science and Technology Development Fund (STDF), Egypt and is gratefully acknowledged.

REFERENCES

[1] Jiaxin Li, Ping Wang, Liying Zhou and Miao Cheng, *ISIJ International*, vol. 47, No. 8, pp. 1097, 2007.
[2] P. J. Meschter and H. J. Grabke, *Metallurgical Transactions B*, vol. 10B, pp. 323, 1979.
[3] Takeaki Murayama, Koichiro Higashi, Kohei Imanishi and Yoichi Ono, *ISIJ international*, vol. 78, No. 7, 1992.
[4] Hideki Ono-Nakazato, Tashinari Yonezawa and Tateo Usui, *ISIJ international*, vol. 43, No. 10, pp. 1502, 2003.
[5] Fengman Shen, Reijiro Takahashi and Jun-ichiro Tagi, ISIJ *International*, vol. 76, No. 4, pp. 523, 1990.
[6] A. A. El-Geassy, M. I. Nasr and M. Bahgat, *Ironmaking Steelmaking*, vol. 27, No. 2, pp. 117, 2000.
[7] B. D. Cullity and S. R. Stock, *Elements of X-Ray Diffraction*, 3rd edition, Prentice Hall, pp. 167, 2001.
[8] M. I. Nasr, A. A. Omar, M. H. Khadr and A. A. El-Geassy, *ISIJ International*, vol. 35, pp. 1043, 1995.
[9] J. Szekely, J. W. Evans and H. Y. Sohn, *Gas-Solid Reaction*, Academic press, N. Y, 1976.
[10] H. Y. Sohn and Szekely, *Chem. Eng. Sci*., vol. 27, pp. 763, 1972.
[11] B. L. Seth and H. U. Ross, *AIME*, vol. 233, pp. 180, 1965.
[12] W. M. Mc Kewan, *AIME*, vol. 218, pp. 2, 1960.